Journal of Financial Econometrics Advance Access published April 9, 2014

Journal of Financial Econometrics, 2014, Vol. 0, No. 0, 1–34

Estimating Shadow-Rate Term Structure Models with Near-Zero Yields

JENS H. E. CHRISTENSEN and GLENN D. RUDEBUSCH
Federal Reserve Bank of San Francisco

ABSTRACT

Standard Gaussian affine dynamic term structure models do not rule out negative nominal interest rates—a conspicuous defect with yields near zero in many countries. Alternative shadow-rate models, which respect the nonlinearity at the zero lower bound, have been rarely used because of the extreme computational burden of their estimation. However, by valuing the call option on negative shadow yields, we provide estimates of a three-factor shadow-rate model of Japanese yields. We validate our option-based results by closely matching them using a simulation-based approach. We also show that the shadow short rate is sensitive to model fit and specification. (*JEL*: G12, E43, E52, E58)

KEYWORDS: affine dynamic term structure models, zero lower bound, monetary policy

Nominal yields on government debt in several countries have fallen very near their zero lower bound (ZLB). Notably, yields on Japanese government bonds of various maturities have been near zero since 1996. Similarly, many U.S. Treasury rates edged down quite close to zero in the years following the financial crisis in late 2008. Accordingly, understanding how to model the term structure of interest rates when some of those interest rates are near the ZLB commands attention for bond portfolio pricing, risk management, for macroeconomic and monetary policy

The views in this paper are solely the responsibility of the authors and should not be interpreted as reflecting the views of the Federal Reserve Bank of San Francisco or the Board of Governors of the Federal Reserve System. We thank Peter Feldhütter, Don Kim, Leo Krippner, and David Lando for helpful comments on previous drafts of this article. We also thank participants at the FDIC's 23rd Annual Derivatives Securities & Risk Management Conference and the NBER Summer Institute 2013 as well as seminar participants at the Copenhagen Business School, the Swiss National Bank, the Office of Financial Research, the Federal Reserve Board, and the Federal Reserve Bank of San Francisco for helpful comments.
Address correspondence to Jens H. E. Christensen, Federal Reserve Bank of San Francisco, 101 Market Street MS 1130, San Francisco,CA 94105, or e-mail: jens.christensen@sf.frb.org

doi:10.1093/jjfinec/nbu010

analysis. Unfortunately, the workhorse representation in finance for bond pricing—the affine Gaussian dynamic term structure model—ignores the ZLB and routinely places positive probabilities on future negative interest rates. This counterfactual flaw stems from ignoring the existence of currency, which is a readily available store of value. In the real world, an investor always has the option of holding cash, and the zero nominal yield of cash will dominate any security with a negative yield.[1]

To recognize the option value of currency in bond pricing, Black's (1995) introduced the notion of a "shadow short rate," which is driven by fundamentals and can be positive or negative. The observed short rate equals the shadow short rate except that the former is bounded below by zero. While Black's (1995) use of a shadow short rate to account for the presence of currency holds much intuitive appeal, it has rarely been used. In part, this infrequency reflects the fact that interest rates in many countries have long been some distance above zero, so the Gaussian models' positive probabilities on negative future interest rates are negligible and unlikely to be an important determinant in bond pricing. In recent years, with yields around the world at historic lows, this rationale no longer applies. However, a second factor limiting the adoption of the shadow-rate structure has been the difficulty in estimating these nonlinear models. Gorovoi and Linetsky (2004) derive quasi-analytical bond price formulas for the case of one-factor Gaussian and square-root shadow-rate models.[2] Unfortunately, their results do not extend to multidimensional models. Instead, the small set of previous research on shadow-rate models has relied on numerical methods for pricing.[3] However, in light of the computational burden of these methods, previous estimations of shadow-rate models have focused on models that use only one or two factors. For example, Ichiue and Ueno (2007) and Kim and Singleton (2012) undertake a full maximum-likelihood estimation of a two-factor Gaussian shadow-rate model on Japanese bond yield data using the extended Kalman filter and numerical optimization. These analyses were limited to only two pricing factors because the numerical methods required for shadow-rate models with more than two factors were computationally too onerous. This practical shortcoming is potentially quite serious given the prevalence of higher-dimensional bond pricing models in research and industry.[4] Indeed, to overcome the practical difficulties of empirical implementation, Ichiue and Ueno (2013) simplify the structure by ignoring bond

[1] Actually, the ZLB can be a somewhat soft floor. The nonnegligible costs of transacting in and holding large amounts of currency have allowed yields to push slightly below zero in a few countries, notably in Denmark recently. To account for institutional currency frictions in our analysis, we could replace the zero lower bound on yields with some appropriate, possibly time-varying, negative epsilon as detailed in Section 2.4.

[2] Ueno et al. (2006) use these formulas when calibrating a one-factor Gaussian model to a sample of Japanese government bond yields.

[3] Kim and Singleton (2012) and Bomfim (2003) use finite-difference methods to calculate bond prices, while Ichiue and Ueno (2007) employ interest rate lattices.

[4] Indeed, Kim and Singleton (2012) suggest that the shadow-rate model results of Ueno et al. (2006) are influenced by their use of a *one*-factor shadow-rate model that may not be flexible enough to fit their sample of Japanese data. Similarly, the Kim and Singleton (2012) two-factor results may not generalize to

convexity effects, so the magnitude of the resulting deviations from arbitrage-free pricing is unclear.

An alternative option-based approach to reduce the computational burden associated with the ZLB, suggested by Krippner (2012), appears to allow for tractable estimation of dynamic term structure shadow-rate models with more than two factors. The intuition for the option-based approach is that the price of a standard observed bond (which is constrained by the ZLB) should equal the price of a shadow-rate bond (which is not constrained by the ZLB) *minus* the price of a call option pertaining to the possibility that the unconstrained shadow rates may go negative. That is, the owner of a shadow bond would have to sell off the probability mass associated with the shadow (zero-coupon) bond trading above par in order to match the value of the observed bond. Unfortunately, this call option is difficult to value, so Krippner (2012) provides only an approximate solution to the correct one. Krippner suggests that the approximation error is likely small, but little is known in practice about its size and properties.

In this article, we implement this new option-based approach to estimate the first three-factor shadow-rate model on Japanese yield data.[5] Specifically, we use the option-based method to estimate a shadow-rate version of the Gaussian arbitrage-free Nelson-Siegel (AFNS) model introduced in Christensen, Diebold, and Rudebusch (2011), henceforth CDR. The AFNS model class provides a flexible and robust structure for dynamic term structure modeling that has performed well on a variety of yield samples by combining good fit with tractable estimation. Furthermore, as we show in this article, with an option-based estimation approach, the AFNS specification of the pricing factor dynamics leads to analytical formulas for the instantaneous shadow forward rates. These new closed-form expressions facilitate straightforward empirical implementation of higher-order shadow-rate models. We demonstrate this with an estimation of shadow-rate AFNS models using Japanese term structure data, which are of special interest because they include a long period of near-zero yields. In particular, we estimate one-, two-, and three-factor versions of the shadow-rate AFNS model and compare these to one-, two-, and three-factor versions of the standard Gaussian AFNS model. We find that shadow-rate models can provide better fit as measured by in-sample metrics such as the RMSEs of fitted yields and the likelihood values. Still, it is evident from these in-sample results that a standard three-factor Gaussian dynamic term structure model—like our Gaussian three-factor AFNS model—has enough flexibility to fit the cross-section of yields fairly well at each point in time even when the shorter end of the yield curve is flattened out at the ZLB. However,

higher-order models. Finally, note that Bauer and Rudebusch (2013) argue that additional macroeconomic factors will be especially useful at the ZLB to augment the standard yields-only model.

[5] Wu and Xia (2013) derive a discrete-time version of the Krippner framework and implement a three-factor specification using U.S. Treasury data. In related research, Priebsch (2013) derives a second-order approximation to the Black (1995) shadow-rate model and estimates a three-factor version thereof, but it requires the calculation of a double integral in contrast to the single integral needed to fit the yield curve in the Krippner framework.

it is not the case that the Gaussian model can account for all aspects of the term structure at the ZLB. Indeed, we show that our estimated three-factor Gaussian model clearly fails along two dimensions. First, despite fitting the yield curve, the model cannot capture the dynamics of yields at the ZLB. One stark indication of this is the high probability the model assigns to negative future short rates—obviously a poor prediction. Second, the standard model misses the compression of yield volatility that occurs at the ZLB as expected future short rates are pinned near zero, longer-term rates fluctuate less. The shadow-rate model, even without incorporating stochastic volatility, can capture this effect.

We then examine three features of the shadow-rate model in detail. As noted above, the option-based approach provides only an approximation to a fully consistent arbitrage-free dynamic term structure model. For our three-factor shadow-rate AFNS model, we compare the option-based approximation to simulation-based results and find that they are very close. Indeed, the option-based approximation errors are typically an order of magnitude smaller than the in-sample fitted errors, so the potential loss from using an option-based approach in a realistic setting like ours appears to be minimal. Second, we assess the efficiency of the extended Kalman filter we use in estimating shadow-rate models by comparing the results to those obtained with the unscented Kalman filter. The results indicate that extended versus unscented filtering makes very little difference, even for our sample of near-zero Japanese yields, which is very promising as the extended Kalman filter is less computationally intensive. Third, we examine the robustness to model specification of the shadow short rate, which has been recommended by some to be a useful measure of the stance of monetary policy at the ZLB (e.g., Krippner 2012, 2013b; Bullard, 2012). We find that there is notable disagreement about the value of the shadow short rate across models with different numbers of factors. This sensitivity to model specification suggests that conclusions based on the shadow short rate near the zero boundary are likely to be fragile.

Finally, we should mention two alternative frameworks to modeling yields near the ZLB that guarantee positive interest rates: stochastic-volatility models with square-root processes and Gaussian quadratic models. Both of these approaches suffer from the theoretical weakness that they treat the ZLB as a reflecting barrier and not as an absorbing one as in the shadow-rate model. Empirically, of course, the recent prolonged periods of very low interest rates seem more consistent with an absorbing state. In addition, Dai and Singleton (2002) disparage the fit of stochastic-volatility models, while Kim and Singleton (2012) compare quadratic and shadow-rate empirical representations and find a slight preference for the latter. Still, we consider all three modeling approaches to be worthy of further investigation, but we view the shadow-rate model to be of particular interest because away from the ZLB it reduces exactly to the standard Gaussian affine model, which is by far the most popular dynamic term structure model. Therefore, the entire voluminous literature on affine models remains completely applicable and relevant when given a modest shadow-rate tweak to handle the ZLB.

The rest of the article is structured as follows. Section 2 introduces the shadow-rate framework and the option-based approach. Section 3 details our shadow-rate AFNS model. Section 4 describes our Japanese yield data. Section 5 presents our empirical findings for one-, two-, and three-factor shadow-rate models. Finally, Section 6 concludes. Two appendices provide technical details on model estimation and detailed model estimation results.

1 SHADOW-RATE MODELS

In this section, we introduce two types of shadow-rate term structure models. The first is the original approach offered by Black (1995). The second is the option-based approach introduced in Krippner (2012).

1.1 The Black Shadow-Rate Model

The concept of a shadow interest rate as a modeling tool to account for the ZLB can be attributed to Black (1995). He noted that the observed nominal short rate will be nonnegative because currency is a readily available asset to investors that carries a nominal interest rate of zero. Therefore, the existence of currency sets a zero lower bound on yields.

To account for this ZLB, Black postulated as a modeling tool a shadow short rate, s_t, that is unconstrained by the ZLB. The usual observed instantaneous risk-free rate, r_t, which is used for discounting cash flows when valuing securities, is then given by the greater of the shadow rate or zero:

$$r_t = \max\{0, s_t\}. \tag{1}$$

Accordingly, as s_t falls below zero, the observed r_t simply remains at the zero bound.

While Black (1995) described circumstances under which the zero bound on nominal yields might be relevant, he did not provide specifics for implementation. Gorovoi and Linetsky (2004) derive one-factor shadow-rate model bond price formulas, which Ueno et al. (2006) use to calibrate a one-factor Gaussian shadow-rate model to Japanese yield data, but these formulas do not generalize to multifactor models. Instead, previous researchers have employed numerical methods for pricing. Bomfim (2003) use finite-difference methods to calculate bond prices, while Ichiue and Ueno (2007) employ interest rate lattices. Kim and Singleton (2012) provide a comprehensive analysis of this type and implement two-factor affine Gaussian and quadratic Gaussian shadow-rate models.

Kim and Singleton (2012) derive the partial differential equation (PDE) that bond prices must satisfy under the restriction that the risk-free rate used for discounting is the greater of the shadow rate or zero,

$$\frac{\partial P}{\partial \tau} - \frac{1}{2} tr\left(\frac{\partial^2 P}{\partial x \partial x} \Sigma \Sigma'\right) - \frac{\partial P}{\partial x} K^{Q}(\theta^{Q} - x) + \max\{0, s(x)\} P = 0, \quad P(0,x) = 1. \tag{2}$$

They solve this PDE using a finite-difference method. Unfortunately, for more than two factors, such numerical methods render it very difficult to solve the associated higher-dimensional PDE systems within a reasonable time.[6] This is a severe limitation to estimating shadow-rate models since the bond pricing literature has focused on models with at least three factors driving bond yields.

1.2 Option-Based Shadow-Rate Models

To overcome the curse of dimensionality that limits numerical-based estimation of shadow-rate models, Krippner (2012) suggested an alternative option-based approach that could make shadow-rate models almost as easy to estimate as the corresponding non-shadow-rate model. In particular, estimation of option-based shadow-rate models with more than two state variables could be tractable.

To illustrate this new approach, consider two bond-pricing situations that differ only because one has a currency in circulation that has a constant nominal value and no transaction costs, while the other has no currency. In the world without currency, the price of a shadow-rate zero-coupon bond, $P(t,T)$, may trade above par, as its risk-neutral expected instantaneous return equals the risk-free shadow short rate, s_t, which may be negative.[7] In contrast, in the world with currency, the price at time t for a zero-coupon bond that pays \$1 when it matures at time T is given by $\underline{P}(t,T)$. This price will never rise above par, so nonnegative yields will never be observed. Consider the relationship between the two bond prices at time t for the shortest (say, overnight) maturity available, δ. In the presence of currency, investors can either buy the zero-coupon bond at price $P(t,t+\delta)$ and receive one unit of currency the following day or just hold the currency. As a consequence, this bond price, which would equal the shadow bond price, must be capped at 1:

$$\begin{aligned}\underline{P}(t,t+\delta) &= \min\{1, P(t,t+\delta)\} \\ &= P(t,t+\delta) - \max\{P(t,t+\delta)-1, 0\}.\end{aligned}$$

That is, the availability of currency implies that the overnight claim has a value equal to the zero-coupon shadow bond price minus the value of a call option on the zero-coupon shadow bond with a strike price of 1. More generally, we can express the price of a bond in the presence of currency as the price of a shadow bond minus the call option on values of the bond above par:

$$\underline{P}(t,T) = P(t,T) - C^A(t,T,T;1), \tag{3}$$

[6] Richard (2013) goes beyond Kim and Singleton (2012) and presents a second-order approximation to a three-factor Black (1995) model using a four-dimensional lattice grid with more than 10 million nodes, and even then any instantaneous correlation between the state variables has to be ignored to calculate bond prices.

[7] The modeling approach with unobserved, or "shadow," components has an analogy in the corporate credit literature. There, it is frequently assumed that the asset value process of a firm exists but is unobserved. Instead, prices of the firm's equity and corporate debt, which can be interpreted as derivatives written on the firm's assets (see Merton, 1974), are used to draw inferences about the asset value process.

where $C^A(t,t,T;1)$ is the value of an American call option at time t with maturity T and strike price 1 written on the shadow bond maturing at T. In essence, in a world with currency, the bond investor has had to sell off the possible gain from the bond rising above par at any time prior to maturity.

Unfortunately, analytically valuing this American option is complicated by the difficulty in determining the early exercise premium. However, Krippner (2012) argues that there is an analytically close approximation based on tractable European options.[8] Specifically, he argues that the above discussion suggests that the last incremental forward rate of any bond will be nonnegative due to the future availability of currency in the immediate time prior to its maturity. As a consequence, he introduces the following auxiliary bond price equation

$$P_a(t,T,T+\delta) = P(t,T+\delta) - C^E(t,T,T+\delta;1), \tag{4}$$

where $C^E(t,T,T+\delta;1)$ is the value of a European call option at time t with maturity T and strike price 1 written on the shadow discount bond maturing at $T+\delta$. It should be stressed that $P_a(t,T,T+\delta)$ is not identical to the bond price $\underline{P}(t,T)$ in Equation (3) whose yield observes the zero lower bound.

The key insight is that the last incremental forward rate of any bond will be nonnegative due to the future availability of currency in the immediate time prior to its maturity. By letting $\delta \to 0$, this idea is taken to its continuous limit, which identifies the corresponding nonnegative instantaneous forward rate:

$$\underline{f}(t,T) = \lim_{\delta \to 0} \left[-\frac{d}{d\delta} P_a(t,T,T+\delta) \right]. \tag{5}$$

Now, the discount bond prices whose yields observe the zero lower bound are approximated by

$$\underline{P}^{app.}(t,T) = e^{-\int_t^T \underline{f}(t,s)ds}. \tag{6}$$

The auxiliary bond price drops out of the calculations, and we are left with formulas for the nonnegative forward rate, $\underline{f}(t,T)$, that are solely determined by the properties of the shadow rate process s_t. Specifically, Krippner (2012) shows that

$$\underline{f}(t,T) = f(t,T) + z(t,T),$$

where $f(t,T)$ is the instantaneous forward rate on the shadow bond, which may go negative, while $z(t,T)$ is given by

$$z(t,T) = \lim_{\delta \to 0} \left[\frac{d}{d\delta} \left\{ \frac{C^E(t,T,T+\delta;1)}{P(t,T)} \right\} \right].$$

In addition, it holds that the observed instantaneous risk-free rate respects the nonnegativity equation (1) as in the Black (1995) model.

[8] Krippner (2012, 2013a) describes the option-based shadow-rate framework as a portfolio of a continuum of European options, unlike our description based on a single American option, but the ultimate pricing formula is the same.

Finally, yield-to-maturity is defined the usual way as

$$\begin{aligned}\underline{y}(t,T) &= \frac{1}{T-t}\int_t^T \underline{f}(t,s)ds \\ &= \frac{1}{T-t}\int_t^T f(t,s)ds + \frac{1}{T-t}\int_t^T \lim_{\delta\to 0}\Big[\frac{\partial}{\partial\delta}\frac{C^E(t,s,s+\delta;1)}{P(t,s)}\Big]ds \\ &= y(t,T) + \frac{1}{T-t}\int_t^T \lim_{\delta\to 0}\Big[\frac{\partial}{\partial\delta}\frac{C^E(t,s,s+\delta;1)}{P(t,s)}\Big]ds.\end{aligned}$$

It follows that bond yields constrained at the ZLB can be viewed as the sum of the yield on the unconstrained shadow bond, denoted $y(t,T)$, which is modeled using standard tools, and an add-on correction term derived from the price formula for the option written on the shadow bond that provides an upward push to deliver the higher nonnegative yields actually observed. Importantly, the result above is general and applies to any assumptions made about the dynamics of the shadow-rate process. However, in reality, as implementation requires the calculation of the limit term under the integral, the option-based shadow-rate models are limited to the Gaussian model class.

It is important to stress that since the observed discount bond prices defined in Equation (6) differ from the auxiliary bond price defined in Equation (4) and used in the construction of the nonnegative forward rate in Equation (5), the option-based framework should be viewed as not fully internally consistent and simply an approximation to an arbitrage-free model.[9] Of course, away from the ZLB, with a negligible call option, the model will match the standard arbitrage-free term structure representation.

Some may find the lack of a theoretically airtight option-based arbitrage-free formulation disconcerting. However, this feature should be put in context of the rest of the shadow-rate modeling literature, which is invariably plagued by approximation. Although many empirical shadow-rate term structure papers start with a theoretically consistent model, various simplifications are made to facilitate empirical implementation. For example, Ichiue and Ueno (2013) start with a rigorous framework, but in their estimation, they omit Jensen's inequality terms to obtain a solution. Alternatively, Kim and Singleton (2012) rigorously solve a PDE using a finite-difference method, but the numerical burden restricts their results to a two-factor model, which is widely considered too parsimonious to be realistic. In implementing the option-based approach, we keep in mind the adage: "There are no true models—only useful ones." Thus, the question becomes how good

[9] In particular, there is no explicit PDE that bond prices must satisfy, including boundary conditions, for the absence of arbitrage as in Kim and Singleton (2012) and shown in Equation (2). An additional source of discrepancy between the option-based framework and Black's shadow-rate model is the fact that all discounting in the former is done with the shadow rate, while, in the latter, it is done with the constrained short rate in equation (1), see Krippner (2013a) for a discussion.

the option-based shadow-rate approximation is near the ZLB. Krippner (2012) compares the option-based results to analytical ones for a calibrated Gaussian one-factor model, and suggests that the approximation can be quite good. We go further and examine this issue in the context of an estimated three-factor model below. While analytical results are not available for a three-factor model comparison, we use simulation-based results as a benchmark and find that the approximation error is quite small.

2 THE SHADOW-RATE AFNS MODEL

In this section, we consider a Gaussian model that leads to tractable formulas for bond yields in the option-based shadow-rate framework. To model the risk-free shadow rate, we employ the affine arbitrage-free class of Nelson–Siegel term structure models derived in CDR. This class of models is very tractable to estimate and has good in-sample fit and out-of-sample forecast accuracy.[10] Here, we extend the AFNS model to incorporate a nonnegativity constraint on observed yields.

2.1 The Standard AFNS(3) Model

We first briefly describe the standard three-factor AFNS(3) model, which ignores the ZLB on yields. In this class of models, the risk-free rate, which we take to be the potentially unobserved shadow rate, is given by

$$s_t = X_t^1 + X_t^2,$$

while the dynamics of the state variables (X_t^1, X_t^2, X_t^3) used for pricing under the Q-measure have the following structure:[11]

$$\begin{pmatrix} dX_t^1 \\ dX_t^2 \\ dX_t^3 \end{pmatrix} = - \begin{pmatrix} 0 & 0 & 0 \\ 0 & \lambda & -\lambda \\ 0 & 0 & \lambda \end{pmatrix} \begin{pmatrix} X_t^1 \\ X_t^2 \\ X_t^3 \end{pmatrix} dt + \begin{pmatrix} \sigma_{11} & 0 & 0 \\ \sigma_{21} & \sigma_{22} & 0 \\ \sigma_{31} & \sigma_{32} & \sigma_{33} \end{pmatrix} \begin{pmatrix} dW_t^{1,Q} \\ dX_t^{2,Q} \\ dX_t^{3,Q} \end{pmatrix}. \tag{7}$$

The AFNS model dynamics under the Q-measure may appear restrictive, but CDR show this structure coupled with general risk pricing provides a very flexible

[10] See, for example, the discussion and references in Diebold and Rudebusch (2013).

[11] We have fixed the mean under the Q-measure at zero and assumed a lower triangular structure for the volatility matrix, which comes at no loss of generality, as described by CDR. As discussed in CDR, with a unit root in the level factor under the pricing probability measure, the model is not arbitrage-free with an unbounded horizon; therefore, as is often done in theoretical discussions, an arbitrary maximum horizon is imposed.

modeling structure. Indeed, CDR demonstrate that this specification implies zero-coupon bond yields that have the popular Nelson and Siegel (1987) factor loading structure,

$$y(t,T)=X_t^1+\Big(\frac{1-e^{-\lambda(T-t)}}{\lambda(T-t)}\Big)X_t^2+\Big(\frac{1-e^{-\lambda(T-t)}}{\lambda(T-t)}-e^{-\lambda(T-t)}\Big)X_t^3-\frac{A(t,T)}{T-t}.$$

In this formulation, the three factors, X_t^1, X_t^2, and X_t^3, are identified by the loadings as level, slope, and curvature, respectively. The yield function also contains a yield-adjustment term, $\frac{A(t,T)}{T-t}$, that is time invariant and depends only on the maturity of the bond. CDR provide an analytical formula for this term, which under our identification scheme is entirely determined by the volatility matrix.

The corresponding instantaneous forward rates are given by

$$f(t,T)=-\frac{\partial}{\partial T}\ln P(t,T)=X_t^1+e^{-\lambda(T-t)}X_t^2+\lambda(T-t)e^{-\lambda(T-t)}X_t^3+A^f(t,T), \tag{8}$$

where the yield-adjustment term in the instantaneous forward rate function is given by

$$\begin{aligned}
A^f(t,T) &= -\frac{\partial A(t,T)}{\partial T}\\
&= -\frac{1}{2}\sigma_{11}^2(T-t)^2-\frac{1}{2}(\sigma_{21}^2+\sigma_{22}^2)\Big(\frac{1-e^{-\lambda(T-t)}}{\lambda}\Big)^2\\
&\quad -\frac{1}{2}(\sigma_{31}^2+\sigma_{32}^2+\sigma_{33}^2)\Big[\frac{1}{\lambda^2}-\frac{2}{\lambda^2}e^{-\lambda(T-t)}-\frac{2}{\lambda}(T-t)e^{-\lambda(T-t)}\\
&\qquad +\frac{1}{\lambda^2}e^{-2\lambda(T-t)}+\frac{2}{\lambda}(T-t)e^{-2\lambda(T-t)}+(T-t)^2e^{-2\lambda(T-t)}\Big]\\
&\quad -\sigma_{11}\sigma_{21}(T-t)\frac{1-e^{-\lambda(T-t)}}{\lambda}\\
&\quad -\sigma_{11}\sigma_{31}\Big[\frac{1}{\lambda}(T-t)-\frac{1}{\lambda}(T-t)e^{-\lambda(T-t)}-(T-t)^2e^{-\lambda(T-t)}\Big]\\
&\quad -(\sigma_{21}\sigma_{31}+\sigma_{22}\sigma_{32})\Big[\frac{1}{\lambda^2}-\frac{2}{\lambda^2}e^{-\lambda(T-t)}-\frac{1}{\lambda}(T-t)e^{-\lambda(T-t)}+\frac{1}{\lambda^2}e^{-2\lambda(T-t)}\\
&\qquad +\frac{1}{\lambda}(T-t)e^{-2\lambda(T-t)}\Big].
\end{aligned}$$

2.2 Bond Option Prices

To implement the option-based approach to the shadow-rate model, we need the analytical formula for the price of the European call option written on the shadow bond described above.

From standard asset pricing theory it follows that the value of a European call option with maturity T and strike price K written on the zero-coupon bond maturing at $T+\delta$ is given by

$$C^E(t,T,T+\delta;K)=E_t^Q\Big[e^{-\int_t^T s_u du}\max\{P(T,T+\delta)-K,0\}\Big].$$

Unreported calculations show that the value of the European call option within the AFNS(3) model is given by[12]

$$C^E(t,T,T+\delta;K) = P(t,T+\delta)\Phi(d_1)-KP(t,T)\Phi(d_2),$$

where $\Phi(\cdot)$ is the cumulative probability function for the standard normal distribution and

$$d_1=\frac{\ln\left(\frac{P(t,T+\delta)}{P(t,T)K}\right)+\frac{1}{2}v(t,T,T+\delta)}{\sqrt{v(t,T,T+\delta)}} \quad \text{and} \quad d_2=d_1-\sqrt{v(t,T,T+\delta)}$$

with

$$\begin{aligned}
v(t,T,T+\delta) = {} & \sigma_{11}^2\delta^2(T-t)+(\sigma_{21}^2+\sigma_{22}^2)\Big(\frac{1-e^{-\lambda\delta}}{\lambda}\Big)^2\frac{1-e^{-2\lambda(T-t)}}{2\lambda} \\
& +(\sigma_{31}^2+\sigma_{32}^2+\sigma_{33}^2)\Bigg[\Big(\frac{1-e^{-\lambda\delta}}{\lambda}\Big)^2\frac{1-e^{-2\lambda(T-t)}}{2\lambda} \\
& \quad +e^{-2\lambda\delta}\Big[\frac{\delta^2-(T+\delta-t)^2e^{-2\lambda(T-t)}}{2\lambda}+\frac{\delta-(T+\delta-t)e^{-2\lambda(T-t)}}{2\lambda^2}+\frac{1-e^{-2\lambda(T-t)}}{4\lambda^3}\Big] \\
& \quad -\frac{1}{2\lambda}(T-t)^2e^{-2\lambda(T-t)}-\frac{1}{2\lambda^2}(T-t)e^{-2\lambda(T-t)}+\frac{1-e^{-2\lambda(T-t)}}{4\lambda^3} \\
& \quad -\frac{(1-e^{-\lambda\delta})e^{-\lambda\delta}}{\lambda^2}\Big[\delta-(T+\delta-t)e^{-2\lambda(T-t)}+\frac{1-e^{-2\lambda(T-t)}}{2\lambda}\Big] \\
& \quad +\frac{1-e^{-\lambda\delta}}{\lambda^2}\Big[\frac{1-e^{-2\lambda(T-t)}}{2\lambda}-(T-t)e^{-2\lambda(T-t)}\Big] \\
& \quad +\frac{1}{\lambda}\delta e^{-\lambda\delta}\Big[(T-t)e^{-2\lambda(T-t)}-\frac{1-e^{-2\lambda(T-t)}}{2\lambda}\Big] \\
& \quad +\frac{1}{\lambda}e^{-\lambda\delta}\Big[(T-t)^2e^{-2\lambda(T-t)}+\frac{1}{\lambda}(T-t)e^{-2\lambda(T-t)}-\frac{1-e^{-2\lambda(T-t)}}{2\lambda^2}\Big]\Bigg] \\
& +2\sigma_{11}\sigma_{21}\delta(1-e^{-\lambda\delta})\frac{1-e^{-\lambda(T-t)}}{\lambda^2} \\
& +2\sigma_{11}\sigma_{31}\delta\Big[-\frac{1}{\lambda}(T-t)e^{-\lambda(T-t)}-\frac{1}{\lambda}e^{-\lambda\delta}\Big(\delta-(T+\delta-t)e^{-\lambda(T-t)}\Big)+2(1-e^{-\lambda\delta})\frac{1-e^{-\lambda(T-t)}}{\lambda^2}\Big]
\end{aligned}$$

[12]The calculations leading to this result are available from the authors upon request. For European options, the put-call parity applies. As a consequence, the value of European put options written on $P(t,T+\delta)$ can be similarly calculated; see Chen (1992) for details.

$$+(\sigma_{21}\sigma_{31}+\sigma_{22}\sigma_{32})\Bigg[\Big(\frac{1-e^{-\lambda\delta}}{\lambda}\Big)^2\frac{1-e^{-2\lambda(T-t)}}{\lambda}$$
$$+\frac{1}{\lambda^2}e^{-2\lambda\delta}\Big[\delta-(T+\delta-t)e^{-2\lambda(T-t)}+\frac{1-e^{-2\lambda(T-t)}}{2\lambda}\Big]$$
$$+\frac{1}{\lambda^2}\Big[-(T-t)e^{-2\lambda(T-t)}+\frac{1-e^{-2\lambda(T-t)}}{2\lambda}\Big]$$
$$-\frac{1}{\lambda^2}e^{-\lambda\delta}\Big[\delta-(2T+\delta-2t)e^{-2\lambda(T-t)}+\frac{1-e^{-2\lambda(T-t)}}{\lambda}\Big]\Bigg].$$

2.3 The Shadow-Rate B-AFNS(3) Model

We refer to the complete three-factor shadow-rate model as the B-AFNS(3) model.[13] Given the above AFNS(3) shadow-rate process and the price of a shadow bond option, we are now ready to price bonds that observe the nonnegativity constraint in a B-AFNS(3) model.

Krippner (2012) provides a formula for the ZLB instantaneous forward rate, $\underline{f}(t,T)$, that applies to any Gaussian model

$$\underline{f}(t,T)=f(t,T)\Phi\Big(\frac{f(t,T)}{\omega(t,T)}\Big)+\omega(t,T)\frac{1}{\sqrt{2\pi}}\exp\Big(-\frac{1}{2}\Big[\frac{f(t,T)}{\omega(t,T)}\Big]^2\Big),$$

where $f(t,T)$ is the shadow forward rate and $\omega(t,T)$ is related to the conditional variance appearing in the shadow bond option price formula as follows:

$$\omega(t,T)^2=\frac{1}{2}\lim_{\delta\to 0}\frac{\partial^2 v(t,T,T+\delta)}{\partial\delta^2}.$$

Within the B-AFNS(3) model, the formula for the shadow forward rate, $f(t,T)$, is provided by equation (8), while $\omega(t,T)$ takes the following form:[14]

$$\omega(t,T)^2=\sigma_{11}^2(T-t)+(\sigma_{21}^2+\sigma_{22}^2)\frac{1-e^{-2\lambda(T-t)}}{2\lambda}$$
$$+(\sigma_{31}^2+\sigma_{32}^2+\sigma_{33}^2)\Big[\frac{1-e^{-2\lambda(T-t)}}{4\lambda}-\frac{1}{2}(T-t)e^{-2\lambda(T-t)}-\frac{1}{2}\lambda(T-t)^2e^{-2\lambda(T-t)}\Big]$$
$$+2\sigma_{11}\sigma_{21}\frac{1-e^{-\lambda(T-t)}}{\lambda}+2\sigma_{11}\sigma_{31}\Big[-(T-t)e^{-\lambda(T-t)}+\frac{1-e^{-\lambda(T-t)}}{\lambda}\Big]$$
$$+(\sigma_{21}\sigma_{31}+\sigma_{22}\sigma_{32})\Big[-(T-t)e^{-2\lambda(T-t)}+\frac{1-e^{-2\lambda(T-t)}}{2\lambda}\Big].$$

[13] Following Kim and Singleton (2012), the prefix "B-" refers to a shadow-rate model in the spirit of Black (1995), while the number shows the number of state variables. Krippner (2012), 2013b) adopts the prefix CAB for "currency-adjusted bond."

[14] The calculations leading to this result are available from the authors upon request.

Now, the zero-coupon bond yields that observe the ZLB, denoted $\underline{y}(t,T)$, are easily calculated as

$$\underline{y}(t,T)=\frac{1}{T-t}\int_t^T\left[f(t,s)\Phi\Big(\frac{f(t,s)}{\omega(t,s)}\Big)+\omega(t,s)\frac{1}{\sqrt{2\pi}}\exp\Big(-\frac{1}{2}\Big[\frac{f(t,s)}{\omega(t,s)}\Big]^2\Big)\right]ds. \quad (9)$$

As highlighted by Krippner (2012), with Gaussian shadow-rate dynamics, the calculation of zero-coupon bond yields involves only a single integral independent of the factor dimension of the model, which greatly facilitates empirical implementation.

2.4 Nonzero Lower Bound for the Short Rate

In this section, we generalize the model and consider a lower bound for the short rate that may differ from zero, i.e.

$$r_t=\max\{r_{min},s_t\}.$$

A few papers have used a nonzero lower bound for the short rate. In the case of U.S. Treasury yields, Wu and Xia (2013) simply fix the lower bound at 25 basis points. A similar approach is applied to Japanese, UK, and U.S. yields by Ichiue and Ueno (2013).[15] As an alternative, Kim and Priebsch (2013) treat r_{min} as a free parameter to be estimated, and using U.S. Treasury yields, they obtain a value of 14 basis points.

In our setting, to derive the implications for the yield function, we merely change the strike price of the bond option from 1 to $K=e^{-r_{min}\delta}$ in the formulas in Section 1.2. Thus, the general formula for the yield that respects the r_{min} lower bound is given by

$$\underline{y}(t,T)=y(t,T)+\frac{1}{T-t}\int_t^T\lim_{\delta\to 0}\Big[\frac{\partial}{\partial\delta}\frac{C^E(t,s,s+\delta;e^{-r_{min}\delta})}{P(t,s)}\Big]ds.$$

It follows that the forward rate that respects the r_{min} lower bound is[16]

$$\underline{f}(t,T)=r_{min}+(f(t,T)-r_{min})\Phi\Big(\frac{f(t,T)-r_{min}}{\omega(t,T)}\Big)+\omega(t,T)\frac{1}{\sqrt{2\pi}}\exp\Big(-\frac{1}{2}\Big[\frac{f(t,T)-r_{min}}{\omega(t,Ts)}\Big]^2\Big),$$

where the shadow forward rate, $f(t,T)$, and $\omega(t,T)$ remain as before.

However, we remain quite sceptical about the use of a non-zero r_{min}. In part, this is because they have not been well motivated. This is especially true for r_{min} values

[15] For Japan, Ichiue and Ueno (2013) impose a lower bound of 9 basis points from January 2009 to December 2012 and reduce it to 5 basis points thereafter. For the United States, they use a lower bound of 14 basis points starting in November 2009. Finally, for the UK, they assume the standard zero lower bound for the short rate.

[16] The calculations leading to this result are available from the authors upon request.

that are *greater* than the observed yields in the sample (and U.S. Treasury yields have reached a low of −1 basis point in recent years). In addition, our own unreported results indicate that the estimated value of the shadow rate can be very sensitive to the value of r_{min}. Similarly, using U.S. Treasury yields, Bauer and Rudebusch (2013) find that the value of the shadow short rate is quite sensitive across a range of values for r_{min}. Thus, in general, the lower bound for the short rate, r_{min}, should be chosen with care. In the context of our Japanese data, the data indeed suggest that zero is the appropriate lower bound with the lowest one- and two-year yields recorded being 0.0 basis point and 1.3 basis point, respectively, while the six-month yield breaches the zero bound on a few occasions, but is never lower than −2 basis points.

2.5 Market Prices of Risk

So far, the description of the B-AFNS(3) model has relied solely on the dynamics of the state variables under the Q-measure used for pricing. However, to complete the description of the model and to implement it empirically, we will need to specify the risk premiums that connect the factor dynamics under the Q-measure to the dynamics under the real-world (or historical) P-measure. It is important to note that there are no restrictions on the dynamic drift components under the empirical P-measure beyond the requirement of constant volatility. To facilitate empirical implementation, we use the extended affine risk premium developed by Cheridito, Filipović, and Kimmel (2007). In the Gaussian framework, this specification implies that the risk premiums Γ_t depend on the state variables; that is,

$$\Gamma_t = \gamma^0 + \gamma^1 X_t,$$

where $\gamma^0 \in \mathbf{R}^3$ and $\gamma^1 \in \mathbf{R}^{3\times 3}$ contain unrestricted parameters.[17] The relationship between real-world yield curve dynamics under the P-measure and risk-neutral dynamics under the Q-measure is given by

$$dW_t^Q = dW_t^P + \Gamma_t dt.$$

Thus, the P-dynamics of the state variables are

$$dX_t = K^P(\theta^P - X_t)dt + \Sigma dW_t^P, \tag{10}$$

where both K^P and θ^P are allowed to vary freely relative to their counterparts under the Q-measure.

Finally, we note that the model estimation is based on the extended Kalman filter and described in Appendix A.

[17] For Gaussian models, this specification is equivalent to the essentially affine risk premium specification introduced in Duffee (2002).

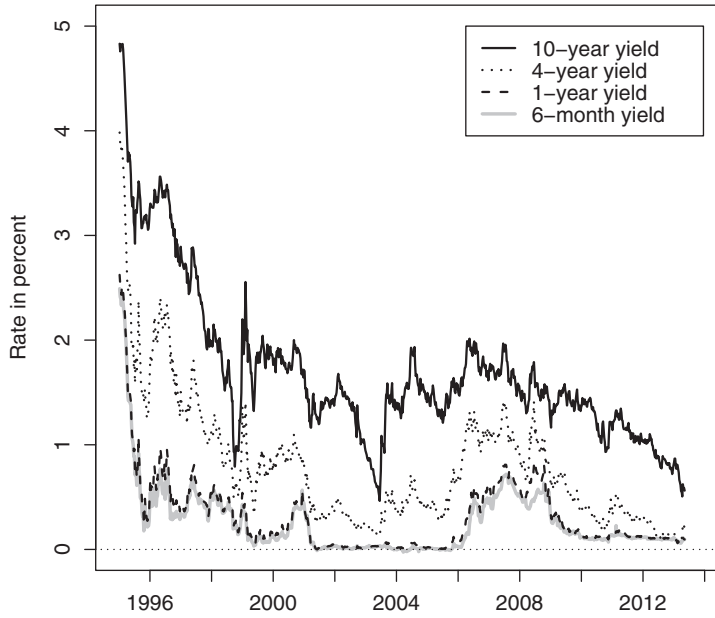

Figure 1 Japanese government bond yields. We show time-series plots of Japanese government bond yields at weekly frequency, at maturities of 6 months, 1 year, 4 years, and 10 years. The data cover the period from January 6, 1995, to May 3, 2013.

3 DATA

The bulk of our sample of Japanese government bond yields is identical to the data set examined by Kim and Singleton (2012).[18] Their data set contains six maturities: six-month yields and one-, two-, four-, seven-, and ten-year yields, and all yields are continuously compounded and measured weekly (Fridays). The Kim and Singleton (2012) sample, however, covers only January 6, 1995, to March 7, 2008, and so ends before the recent global financial crisis episode, which was marked by extremely low bond yields in Japan and in many other countries. This recent episode is extremely interesting to consider from a variety of economic and finance perspectives; therefore, we augment the original Kim and Singleton (2012) sample with Japanese government zero-coupon yields downloaded from Bloomberg through May 3, 2013.[19]

Figure 1 shows the variation over time in four of the six yields. During two periods—from 2001 to 2005 and from 2009 to 2013—six-month and one-year yields are pegged near zero. These episodes are obvious candidates for possible negative shadow rates. As noted by Kim and Singleton (2012), these periods also

[18]We thank Don Kim for sharing these data.

[19]When the two sources of data overlap during 2007 and 2008, the two sets of yields match almost exactly.

Table 1 Factor loadings for Japanese government bond yields

Maturity (months)	Loading on		
	First P.C.	Second P.C.	Third P.C.
6	−0.21	−0.49	0.53
12	−0.23	−0.50	0.25
24	−0.31	−0.43	−0.32
48	−0.45	−0.15	−0.57
84	−0.57	0.33	−0.11
120	−0.53	0.44	0.46
% explained	93.48	5.85	0.51

The first six rows show how bond yields at various maturities load on the first three principal components. The bottom row shows the proportion of all bond yield variability explained by each principal component. The data are weekly Japanese government bond yields from January 6, 1995, to May 3, 2013.

display reduced volatility of short- and medium-term yields due to the zero bound constraint.

Researchers have found that three factors are typically needed to model the time-variation in cross sections of bond yields (e.g., Litterman and Scheinkman, 1991). Indeed, for our sample of Japanese bond yields, 99.84 percent of the total variation is accounted for by three factors. As Table 1 reports, the first principal component loading's across maturities (the associated eigenvector) is uniformly negative, so like a level factor, a shock to this component changes all yields in the same direction irrespective of maturity. The second principal component is a slope factor, as a shock to this component steepens or flattens the yield curve. Finally, the third component has a U-shaped factor loading as a function of maturity, which is naturally interpreted as a curvature factor. This pattern of level, slope, and curvature motivates our use of the Nelson–Siegel level, slope, and curvature factors for modeling Japanese bond yields, even though we emphasize that our estimated state variables are *not* identical to the principal components.

4 RESULTS

In this section, we describe and assess one-, two-, and three-factor empirical shadow-rate models. We first compare the shadow-rate model fit to the data—relative to each other and to non-shadow-rate dynamic term structure models. We also discuss some of the advantages of using Gaussian shadow-rate models over standard Gaussian models in a near-ZLB environment. Next, we evaluate the closeness of the option-based approximation to a matching simulated shadow-rate model, before we study the efficiency of the extended Kalman filter in estimating shadow-rate models. Finally, we examine the sensitivity of the shadow short rate to the number of factors in the model.

4.1 In-sample Fit of Standard and Shadow-Rate Models

We begin by considering the simplest possible case for the shadow-rate dynamics, namely the one-factor Gaussian model of Vasiček (1977). Although this model may seem to be too simple to be of interest, it has been employed by several previous studies[20] and is a useful tool for comparison. In this one-factor case, the factor dynamics of the shadow rate s_t used for pricing under the risk-neutral Q-measure are

$$ds_t = \kappa^Q(\theta^Q - s_t)dt + \sigma dW_t^Q,$$

with the risk-free rate given by the greater of the shadow rate or zero:

$$r_t = \max\{0, s_t\}.$$

The instantaneous forward rate is given by

$$f(t,T) = e^{-\kappa^Q(T-t)}s_t + \theta^Q(1-e^{-\kappa^Q(T-t)}) - \frac{1}{2}\sigma^2\Big(\frac{1-e^{-\kappa^Q(T-t)}}{\kappa^Q}\Big)^2,$$

while

$$\omega(t,T)^2 = \sigma^2\frac{1-e^{-2\kappa^Q(T-t)}}{2\kappa^Q}.$$

Allowing for time-varying risk premiums, the dynamics under the objective P-measure are fully flexible,

$$ds_t = \kappa^P(\theta^P - s_t)dt + \sigma dW_t^P.$$

We refer to this representation inspired by Black (1995) as the B-V(1) model. We also estimate the standard Vasiček (1977) model, denoted as the V(1) model, without the nonnegativity constraint or the shadow-rate interpretation.

Table 2 reports the summary statistics of the fitted errors for the V(1) and B-V(1) models.[21] The better fit of the B-V(1) model across all yield maturities is notable, with an average root mean-squared error (RMSE) improvement of 1.7 basis points. This better fit can also be seen in the higher likelihood value of the B-V(1) model.

To most closely approximate the two-factor Gaussian shadow-rate model of Kim and Singleton (2012),[22] we estimate a two-factor version of the B-AFNS model that has level and slope factors but no curvature factor. This model is characterized by a shadow rate given by

$$s_t = X_t^1 + X_t^2.$$

[20] These include Gorovoi and Linetsky (2004), Ueno, Baba, and Sakurai (2006), and Krippner (2012).
[21] The estimated parameters of all models in this section are provided in Appendix B.
[22] This is their B-AG2 model.

Table 2 Summary statistics of model fit

	Maturity in months							
RMSE	6	12	24	48	84	120	All yields	Max log$L$
One-factor models								
V(1)	5.8	0.0	12.1	32.8	55.6	52.4	34.4	28,362.97
B-V(1)	4.9	0.2	10.9	30.2	52.5	50.8	32.7	29,263.60
Two-factor models								
AFNS(2)	5.9	0.0	9.0	17.6	21.6	0.0	12.2	32,186.23
B-AFNS(2)	6.6	0.3	8.9	14.6	17.0	3.2	10.3	32,808.21
Three-factor models								
AFNS(3)	0.0	2.4	0.2	4.2	0.0	23.3	9.7	35,469.67
B-AFNS(3)	0.4	2.1	0.3	3.5	0.7	16.7	7.0	36,520.00

The table presents the root mean-squared error of the fitted bond yields from one-, two-, and three-factor models estimated on the weekly Japanese government bond yield data over the period from January 6, 1995, to May 3, 2013. All numbers are measured in basis points. The last column reports the obtained maximum log-likelihood values.

The state variables (X_t^1, X_t^2) used for pricing under the risk-neutral Q-measure have the following dynamics:

$$\begin{pmatrix} dX_t^1 \\ dX_t^2 \end{pmatrix} = -\begin{pmatrix} 0 & 0 \\ 0 & \lambda \end{pmatrix}\begin{pmatrix} X_t^1 \\ X_t^2 \end{pmatrix} dt + \begin{pmatrix} \sigma_{11} & 0 \\ \sigma_{21} & \sigma_{22} \end{pmatrix}\begin{pmatrix} dW_t^{1,Q} \\ dX_t^{2,Q} \end{pmatrix}.$$

As for the P-dynamics, we focus on the most flexible specification with full K^P matrix

$$\begin{pmatrix} dX_t^1 \\ dX_t^2 \end{pmatrix} = \begin{pmatrix} \kappa_{11}^P & \kappa_{12}^P \\ \kappa_{21}^P & \kappa_{22}^P \end{pmatrix}\left[\begin{pmatrix} \theta_1^P \\ \theta_2^P \end{pmatrix} - \begin{pmatrix} X_t^1 \\ X_t^2 \end{pmatrix}\right] dt + \begin{pmatrix} \sigma_{11} & 0 \\ \sigma_{21} & \sigma_{22} \end{pmatrix}\begin{pmatrix} dW_t^{1,P} \\ dW_t^{2,P} \end{pmatrix}.$$

This model has a total of ten parameters, two less than the canonical B-AG2 model used by Kim and Singleton (2012). We estimate both the standard version of this model without any constraints related to the ZLB, denoted as the AFNS(2) model, and the corresponding shadow-rate model, denoted as the B-AFNS(2) model.

Table 2 also reports summary statistics for the fit of the two-factor models. The AFNS(2) model performs reasonably well, but the B-AFNS(2) model has smaller yield RMSEs. The fit of the B-AFNS(2) model is comparable to the B-AG2 model estimated in Kim and Singleton (2012) even though the B-AFNS(2) model has fewer parameters under the Q-dynamics used for pricing.[23]

[23] Our RMSEs are very close to our estimated error standard deviations, $\widehat{\sigma}_\varepsilon(\tau_i)$, and to the estimated error deviations reported by Kim and Singleton (2012).

Finally, we extend the analysis to three-factor models. In the AFNS(3) model, the risk-neutral Q-dynamics used for pricing are as detailed in Section 2, while we assume fully flexible factor dynamics under the P-measure:

$$\begin{pmatrix} dX_t^1 \\ dX_t^2 \\ dX_t^3 \end{pmatrix} = \begin{pmatrix} \kappa_{11}^P & \kappa_{12}^P & \kappa_{13}^P \\ \kappa_{21}^P & \kappa_{22}^P & \kappa_{23}^P \\ \kappa_{31}^P & \kappa_{32}^P & \kappa_{33}^P \end{pmatrix} \left[\begin{pmatrix} \theta_1^P \\ \theta_2^P \\ \theta_3^P \end{pmatrix} - \begin{pmatrix} X_t^1 \\ X_t^2 \\ X_t^3 \end{pmatrix} \right] dt + \begin{pmatrix} \sigma_{11} & 0 & 0 \\ \sigma_{21} & \sigma_{22} & 0 \\ \sigma_{31} & \sigma_{32} & \sigma_{33} \end{pmatrix} \begin{pmatrix} dW_t^{1,P} \\ dW_t^{2,P} \\ dW_t^{3,P} \end{pmatrix}.$$

Table 2 reports the summary statistics of the fitted errors of the regular AFNS(3) model as well as its shadow-rate version, B-AFNS(3). Similar to what we observed for the two-factor models, the shadow-rate model outperforms its standard counterpart when it comes to model fit. In comparing model fit across the two- and three-factor models, the AFNS(3) model is on par with the B-AFNS(2) model, while the B-AFNS(3) model has a bit closer fit than either of them.

4.2 Why Use a Shadow-Rate Model?

Before turning to an analysis of the shadow rate models, it is useful to reinforce the basic motivation for our analysis by examining short rate forecasts and volatility estimates from the estimated AFNS(3) model. With regard to short rate forecasts, any standard affine Gaussian dynamic term structure model may place positive probabilities on future negative interest rates. Accordingly, Figure 2 shows the probability obtained from the AFNS(3) model that the short rate three months out will be negative. Over much of the sample, the probabilities of future negative interest rates are negligible. However, near the ZLB—from 1999 to 2005 and from 2009 through the end of our sample—the model is typically predicting substantial likelihoods of impossible realizations.

Another serious limitation of the standard Gaussian model is the assumption of constant yield volatility, which is particularly unrealistic when periods of normal volatility are combined with periods in which yields are greatly constrained in their movements near the ZLB. Again, a shadow-rate model approach can mitigate this failing significantly. Figure 3 shows the implied three-month conditional yield volatility of the two-year yield from the AFNS(3) and B-AFNS(3) models[24] along with a comparison to the three-month realized volatility of the two-year yield calculated from our sample using daily frequency.[25] While the conditional yield volatility from the AFNS(3) model is constant, the conditional yield volatility from the B-AFNS(3) model closely matches the realized volatility series—with a

[24] For the AFNS(3) model conditional yield volatilities can be calculated using the formulas provided in Fisher and Gilles (1996), while conditional yield volatilities in the B-AFNS(3) model must be generated via Monte Carlo simulation.

[25] As in Kim and Singleton (2012), these are the rolling standard deviation of daily yield changes over 60 trading-day windows.

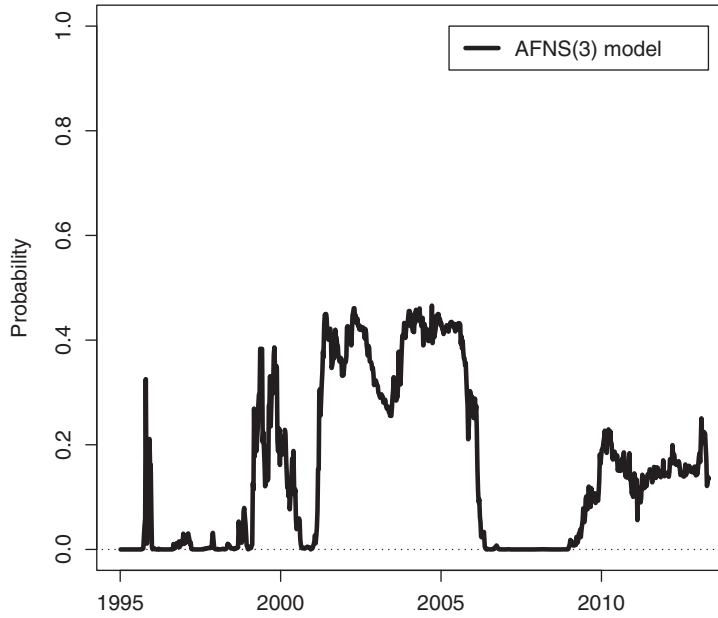

Figure 2 Probability of negative short rates. Illustration of the conditional probability of negative short rates three months ahead from the AFNS(3) model.

correlation of 72 percent. Particularly noteworthy is the B-AFNS(3) model's ability to produce nearzero yield volatility when yields are at their lowest (during 2001–2005 and 2009–2013).

4.3 How Good is the Option-Based Approximation?

As noted above, the option-based approach does not constitute a formal derivation of arbitrage-free pricing relationships, but merely represents an approximation of such relationships. Therefore, in this subsection, we analyze how closely the option-based bond pricing from the estimated B-AFNS(3) model matches an arbitrage-free bond pricing that is obtained from the same model using Black's (1995) approach based on Monte Carlo simulations.

As a motivating comparison, Figure 4 shows analytical and simulation-based yield curves and option-based and simulation-based shadow yield curves from the estimated B-AFNS(3) model as of January 9, 2004—which is during a Japanese ZLB period. The simulation-based shadow yield curve is obtained from 25,000 10-year long factor paths generated using the estimated Q-dynamics of the state variables in the B-AFNS(3) model, which, ignoring the nonnegativity Equation (1), are used to construct 25,000 paths for the shadow short rate. These are converted into a corresponding number of shadow discount bond paths and averaged for each maturity before the resulting shadow discount bond prices are converted into

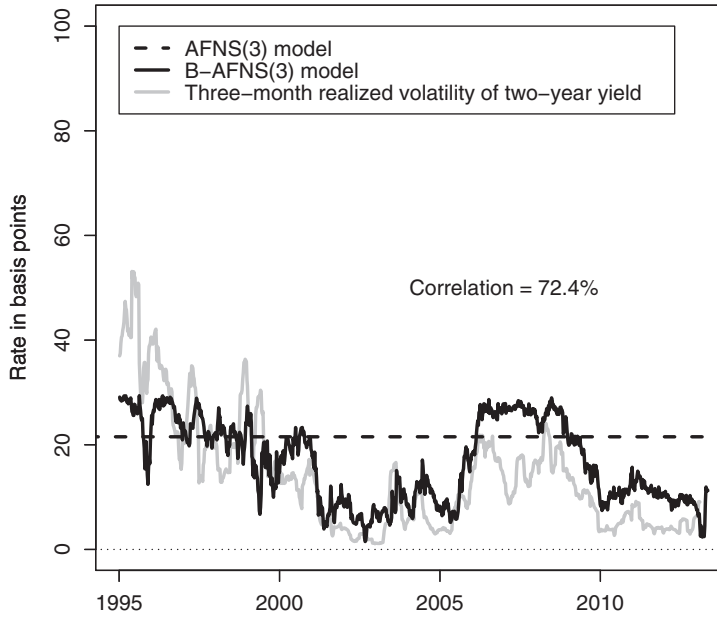

Figure 3 Three-month conditional volatility of two-year yield. Illustration of the three-month conditional volatility of the two-year yield implied by the estimated AFNS(3) and B-AFNS(3) models. Also shown is the subsequent three-month realized volatility of the two-year yield based on daily data.

yields. The simulation-based yield curve is obtained from the same underlying 25,000 Monte Carlo factor paths, but at each point in time in the simulation, the resulting short rate is constrained by the nonnegativity Equation (1) as in Black (1995). The shadow-rate curve from the B-AFNS(3) model can also be calculated analytically via the usual affine pricing relationships, which ignore the ZLB. Note that the simulated shadow yield curve is almost identical to this analytical shadow yield curve. Any difference between these two curves is simply numerical error that reflects the finite number of simulations. More interestingly, the differences between the simulation-based and option-based yield curves are also hard to discern. The minuscule discrepancies between these two yield curves show that the approximation error associated with the option-based approach to calculating bond yields near the ZLB is also very small in this instance.

To document that the close match between the option-based and the simulation-based yield curves is not limited to one specific date, we repeated the simulation exercise for the first observation in each year of our sample. Table 3 reports the resulting shadow yield curve differences and yield curve differences for various maturities on these 19 dates. Again, the errors for the shadow yield curves solely reflect simulation error as the model-implied shadow yield curve is identical to the analytical arbitrage-free curve that would prevail without currency

Table 3 Approximation errors in yields for three-factor model

Dates		Maturity in months 12	36	60	84	120
	Shadow yields	0.10	−0.04	−0.42	−0.67	−0.76
1/2/95	Yields	0.07	−0.09	−0.46	−0.70	−0.61
	Shadow yields	0.37	0.81	1.31	1.68	2.44
1/5/96	Yields	0.33	0.77	1.28	1.69	2.56
	Shadow yields	0.04	0.06	0.19	−0.04	0.14
1/10/97	Yields	0.05	0.10	0.21	0.01	0.72
	Shadow yields	−0.05	−0.22	−0.23	−0.37	−0.95
1/9/98	Yields	−0.02	−0.05	0.07	0.24	1.05
	Shadow yields	0.00	−0.25	−0.34	−0.31	0.23
1/8/99	Yields	−0.02	−0.23	−0.29	−0.10	1.36
	Shadow yields	−0.06	−0.17	0.04	−0.14	−1.02
1/7/00	Yields	−0.07	−0.04	0.39	0.72	1.57
	Shadow yields	0.07	0.58	0.75	0.61	0.06
1/5/01	Yields	0.08	0.56	1.03	1.45	2.58
	Shadow yields	0.14	0.56	0.67	0.45	0.01
1/4/02	Yields	0.08	0.37	0.54	0.82	2.15
	Shadow yields	−0.11	0.31	0.32	0.38	0.60
1/10/03	Yields	0.00	0.26	0.83	1.74	3.97
	Shadow yields	−0.07	−0.26	−0.62	−0.79	−0.25
1/9/04	Yields	−0.05	−0.11	−0.23	0.18	2.36
	Shadow yields	0.19	0.24	0.29	0.31	−0.16
1/7/05	Yields	0.05	0.29	0.83	1.45	2.55
	Shadow yields	0.27	0.27	0.37	0.91	1.91
1/6/06	Yields	0.12	0.25	0.44	1.23	3.28
	Shadow yields	0.18	−0.13	−0.09	−0.09	−0.17
1/6/07	Yields	0.16	−0.13	0.07	0.51	2.23
	Shadow yields	−0.12	−0.03	−0.10	−0.27	−0.12
1/6/08	Yields	−0.12	0.03	0.12	0.40	1.87
	Shadow yields	−0.36	−0.66	−0.34	−0.01	0.58
1/2/09	Yields	−0.28	−0.30	0.20	0.80	2.73
	Shadow yields	0.05	0.14	0.18	0.46	0.69
1/1/10	Yields	−0.03	0.20	0.51	1.26	3.37
	Shadow yields	0.23	−0.21	−0.88	−1.52	−2.44
1/7/11	Yields	0.05	0.07	0.04	0.21	1.36
	Shadow yields	0.06	−0.10	−0.45	−0.40	0.09
1/6/12	Yields	−0.01	−0.05	−0.07	0.56	2.89
	Shadow yields	0.23	0.47	0.76	1.06	1.03
1/4/13	Yields	0.06	0.22	0.62	1.48	3.63
Average	Shadow yields	0.14	0.29	0.44	0.55	0.72
absolute difference	Yields	0.09	0.22	0.43	0.82	2.25

At each date, the table reports differences between the analytical shadow yield curve obtained from the option-based estimates of the B-AFNS(3) model and the shadow yield curve obtained from 25,000 simulations of the estimated factor dynamics under the Q-measure in that model. The table also reports for each date the corresponding differences between the fitted yield curve obtained from the B-AFNS(3) model and the yield curve obtained via simulation of the estimated B-AFNS(3) model with imposition of the ZLB. The bottom two rows give averages of the absolute differences across the 19 dates. All numbers are measured in basis points.

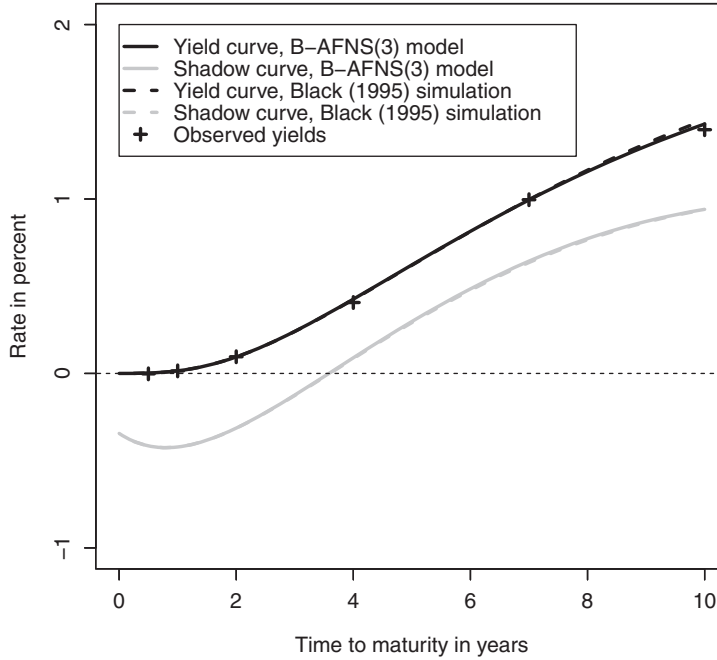

Figure 4 Fitted yield curves in three-factor shadow-rate models. Fitted and shadow yield curves from an option-based estimated B-AFNS(3) model are shown as of January 9, 2004. In addition, the corresponding curves are shown based on a simulation using Black's (1995) approach and $N = 25{,}000$ paths of the state variables drawn using the option-based estimated B-AFNS(3) model factor dynamics under the Q-measure.

in circulation. These simulation errors in Table 3 are typically very small in absolute value, and they increase only slowly with maturity. Their average absolute value—shown in the bottom row—is less than one basis point even at a 10-year maturity. This implies that using simulations with a large number of draws ($N = 25{,}000$) arguably delivers enough accuracy for the type of inference we want to make here.

Given this calibration of the size of the numerical errors involved in the simulation, we can now assess the more interesting size of the approximation error in the option-based approach to valuing yields in the presence of the ZLB. In Table 3, the errors of the fitted B-AFNS(3) model yield curve relative to the simulated results are only slightly larger than those reported for the shadow yield curve. In particular, for maturities up to seven years, the errors tend to be less than 1 basis point, so the option-based approximation error adds very little if anything to the numerical simulation error. At the 10-year maturity, the approximation errors are understandably larger, but even the largest errors at the 10-year maturity do not exceed 4 basis points in absolute value and the average absolute value is around 2 basis points. Overall, the option-based approximation errors in our three-factor

setting appear relatively small. Indeed, they are smaller than the fitted errors described in Table 2. That is, for the B-AFNS(3) model, the gain from using a numerical estimation approach instead of the option-based approximation would in all likelihood be negligible.

Of course, these favorable results on the modest size of the approximation error may not generalize to all situations. We are aware of two other relevant examinations of the option-based approach. First, Krippner (2012) reports approximation errors closer to 6 basis points at the ten-year maturity for a calibrated one-factor Vasiček model.[26] Second, Christensen and Rudebusch (2013) find only a few basis points approximation error for their B-AFNS(3) model estimated on U.S. Treasury yield data.[27] Ultimately, in future applications, we recommend examining the accuracy of the option-based approximation as a routine matter using the simulation-based validation described here. Indeed, we view the ready availability of a validation methodology as a positive feature of the option-based approach. In contrast, the computational burden of the theoretically rigorous approach employed by Kim and Singleton (2012), which requires using a two-factor model as an approximation to what is likely a three-factor data-generating process, does not permit an investigation of the quality of that two-factor approximation.

4.4 How Efficient is the Extended Kalman Filter?

In the literature, various Kalman filtering methods have been used to estimate shadow-rate models. Kim and Singleton (2012) use the standard extended Kalman filter that we also rely upon throughout this paper. Kim and Priebsch (2013) apply the unscented Kalman filter, while Krippner (2013a) uses the iterated extended Kalman filter. In this section, to shed light on the efficiency of the standard extended Kalman filter in estimating shadow-rate models, we re-estimate all three shadow-rate models using the unscented Kalman filter as described in Filipović and Trolle (2013).

Table 4 reports the summary statistics of the fitted errors in the one-, two-, and three-factor shadow-rate models when estimated with both the extended Kalman filter and the unscented Kalman filter. In terms of RMSEs, the differences are barely noticeable. However, using the unscented Kalman filter does produce a marginally better overall fit to the cross section of yields as reflected in the slightly higher maximum log-likelihood values. Furthermore, unreported results show that both the filtered paths and the estimated parameters are barely distinguishable for the same model whether the extended or unscented Kalman filter is used for model estimation.[28] Since the extended Kalman filter is less computationally intensive

[26] Using our Monte Carlo simulation method, we replicated these one-factor results—namely, Table 6.1 of Gorovoi and Linetsky (2004) and Tables 1 and 2 of Krippner (2012).

[27] Wu and Xia (2013) also use simulation-based validation of their U.S. shadow-rate model, which is a discrete-time version of the Krippner framework, and report similar approximation errors.

[28] These results are available from the authors upon request.

Table 4 Summary statistics of model fit

	Maturity in months							
RMSE	6	12	24	48	84	120	All yields	Max log$L$
B-V(1) model								
Extended KF	4.9	0.2	10.9	30.2	52.5	50.8	32.7	29,263.60
Unscented KF	5.0	0.2	10.8	30.2	52.4	50.8	32.6	29,279.22
B-AFNS(2) model								
Extended KF	6.6	0.3	8.9	14.6	17.0	3.2	10.3	32,808.21
Unscented KF	6.7	0.4	8.8	14.5	17.0	3.2	10.3	32,815.83
B-AFNS(3) model								
Extended KF	0.4	2.1	0.3	3.5	0.7	16.7	7.0	36,520.00
Unscented KF	0.4	2.2	0.3	3.5	0.4	16.7	7.0	36,528.49

The table presents the root mean-squared error of the fitted bond yields from one-, two-, and three-factor models estimated on the weekly Japanese government bond yield data over the period from January 6, 1995, to May 3, 2013. All numbers are measured in basis points. The last column reports the obtained maximum log-likelihood values.

than the unscented Kalman filter (the expensive yield function must be evaluated less times in each time step), but still delivers almost identical results, we conclude that the extended Kalman filter is efficient at estimating shadow-rate models, even when yields are as low as in our sample where, presumably, the nonlinearity from the zero lower bound would pose the biggest challenge.[29]

4.5 Shadow Short Rate Comparisons Across Models

Finally, we examine estimates of the shadow short rate, which has been recommended by some to be a useful measure of the stance of monetary policy at the ZLB (e.g., Bullard, 2012; Krippner, 2012, 2013b). Figure 5 shows the instantaneous shadow short-rate paths implied by our one-, two-, and three-factor shadow-rate models. Also, for comparison, we include the shadow-rate path from the B-AG2 model as estimated by Kim and Singleton (2012) for their sample from January 6, 1995, to March 7, 2008. The pairwise correlations between the estimated shadow-rate paths range from 0.887 to 0.993. There is little disagreement across models when the instantaneous rate is in positive territory; however, when the shadow rate is negative, there can be pronounced differences among the levels of the estimated shadow short rates across the one-, two-, and three-factor models, with the shadow short rate from the B-AFNS(3) model generally the least negative. Furthermore, we have found that even within each model class, there can be disagreement across

[29] This conclusion is consistent with the findings of Christoffersen et al. (2013), who conclude that, when states are extracted from securities that are only mildly nonlinear in the state variables, such as interest rate swaps, the extended Kalman filter is adequate.

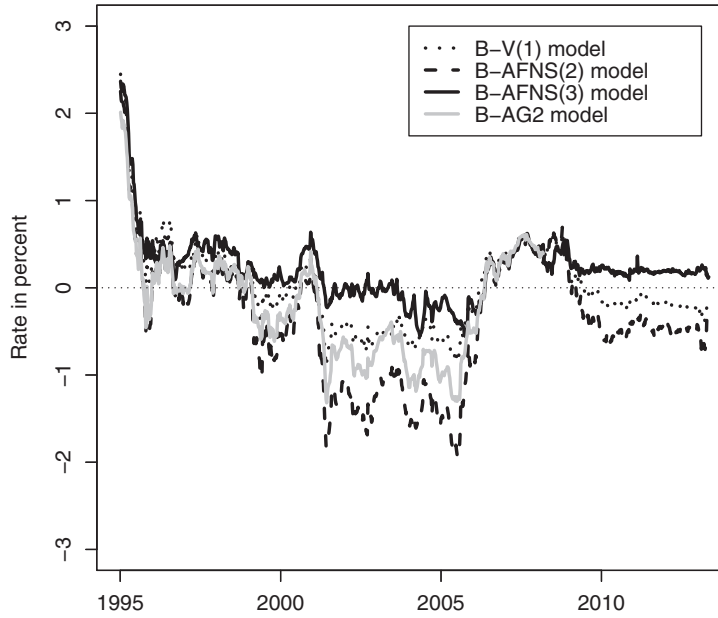

Figure 5 Model-implied shadow rates. Illustration of the model-implied shadow rate from the B-V(1), B-AFNS(2), and B-AFNS(3) models. For comparison, we include the B-AG2 model shadow rate estimated by Kim and Singleton (2012) through 2008.

specifications about how negative the shadow rate is depending on the parsimony of the model.[30]

To further illustrate the source of the sensitivity of the shadow short rates to model specification, we examine the two- and three-factor model fit on a specific date, July 1, 2005, when the shadow rate attains a very low value according to most models shown in Figure 5. Figure 6a illustrates observed yields on this date as well as fitted yield curves from the AFNS(2) and B-AFNS(2) models, while Figure 6b shows the corresponding output for the AFNS(3) and B-AFNS(3) models. For the two-factor models, we note that the AFNS(2) model has difficulty matching the kink in the observed yields around the two-year maturity point, which is very pronounced during this period. On the other hand, for the three-factor models, this distinction between standard and shadow-rate models is much less apparent. It appears that the plain-vanilla AFNS(3) model has sufficient flexibility to handle the kink even on this very challenging day in the sample.

[30]The diversity in our shadow short rates can be compared to other studies. Ueno, Baba, and Sakurai (2006) calibrate one-factor version of the Black (1995) model on Japanese data and calculate a shadow short rate that is typically lower than −5 percent, with the lowest reading falling below −15 percent in the summer of 2002. Ichiue and Ueno (2007) use the Kalman filter to estimate a two-factor shadow-rate model on monthly Japanese government bond yields and report shadow-rate values in a range from −1 to −0.5 percent for the 2001–2005 period.

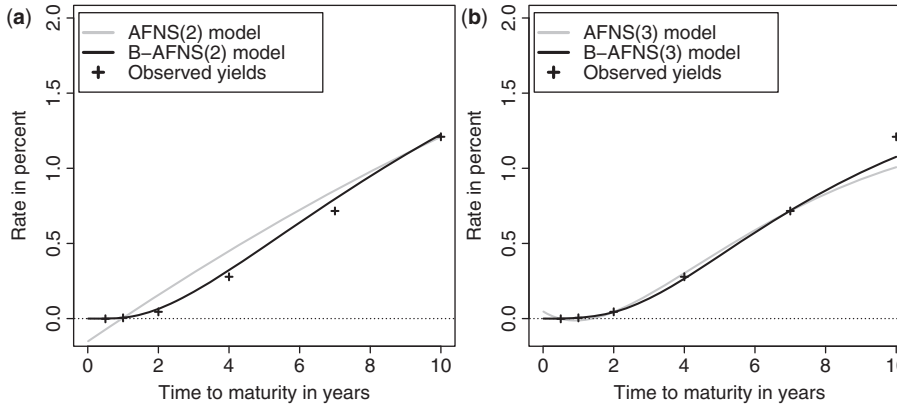

Figure 6 Fitted yield curves on July 1, 2005. The figure to the left illustrates the fitted yield curves from the AFNS(2) and B-AFNS(2) models on July 1, 2005. Also shown are the six observed yields on that date. The figure to the right shows the corresponding results for the AFNS(3) and B-AFNS(3) models.

All in all, our results indicate that the shadow short rate is model specific and likely not a useful measure of the stance of monetary policy when yields are near the ZLB. At a minimum, a number of model specifications should be analyzed to verify the robustness of any shadow short rate conclusions.

5 CONCLUSION

To adapt the Gaussian term structure model to the recent near-zero interest rate environment, we have combined the arbitrage-free Nelson–Siegel model dynamics with the option-based shadow-rate methodology of Krippner (2012). We derive the relevant closed-form solution and estimate variants of this model—including the first three-factor shadow-rate model—using near-zero Japanese yields. We find that the option-based B-AFNS(3) shadow-rate model introduced in this article provides a very close approximation to the results one would obtain by using a simulation-based implementation of the same model as originally envisioned by Black (1995). Based on this evidence, we conclude that the option-based shadow-rate model class appears to be competitive for modeling yield curve dynamics in the current near-zero yield environment. A useful next step in future research would be to put this shadow-rate representation to work, say, making interest predictions or valuing derivatives at the ZLB. For this, finding a preferred specification of the shadow rate factor dynamics and dealing with any finite-sample estimation bias is of importance.

Finally, although some have recommended using the shadow short rate as a measure of the stance of monetary policy, we find that estimated shadow short rates

are sensitive to the number of factors included in the estimation. Other aspects of model specification—such as the maturities of yields included in the sample or the ratio of near-ZLB yields to normal yield observations in the sample—would also likely have an important influence on the shadow short rate, and we cannot recommend it as a robust measure.

APPENDIX A: KALMAN FILTER ESTIMATION OF SHADOW-RATE MODELS

In this appendix, we describe the estimation of the shadow-rate models based on the extended Kalman filter.

For affine Gaussian models, in general, the conditional mean vector and the conditional covariance matrix are

$$E^P[X_T|\mathcal{F}_t] = (I-\exp(-K^P\Delta t))\theta^P+\exp(-K^P\Delta t)X_t,$$
$$V^P[X_T|\mathcal{F}_t] = \int_0^{\Delta t} e^{-K^P s}\Sigma\Sigma' e^{-(K^P)'s}ds,$$

where $\Delta t = T-t$. We compute conditional moments of discrete observations and obtain the state transition equation

$$X_t = (I-\exp(-K^P\Delta t))\theta^P+\exp(-K^P\Delta t)X_{t-1}+\xi_t,$$

where Δt is the time between observations. In the standard Kalman filter, the measurement equation would be affine, in which case

$$y_t = A+BX_t+\varepsilon_t.$$

The assumed error structure is

$$\begin{pmatrix}\xi_t\\ \varepsilon_t\end{pmatrix}\sim N\left[\begin{pmatrix}0\\0\end{pmatrix},\begin{pmatrix}Q & 0\\ 0 & H\end{pmatrix}\right],$$

where the matrix H is assumed diagonal, while the matrix Q has the following structure:

$$Q = \int_0^{\Delta t} e^{-K^P s}\Sigma\Sigma' e^{-(K^P)'s}ds.$$

In addition, the transition and measurement errors are assumed orthogonal to the initial state.

Now we consider Kalman filtering, which we use to evaluate the likelihood function.

Due to the assumed stationarity, the filter is initialized at the unconditional mean and variance of the state variables under the P-measure: $X_0 = \theta^P$ and

$\Sigma_0 = \int_0^\infty e^{-K^P s} \Sigma \Sigma' e^{-(K^P)' s} ds$, which we calculate using the analytical solutions provided in Fisher and Gilles (1996).

Denote the information available at time t by $Y_t = (y_1, y_2, \ldots, y_t)$, and denote model parameters by ψ. Consider period $t-1$ and suppose that the state update X_{t-1} and its mean square error matrix Σ_{t-1} have been obtained. The prediction step is

$$X_{t|t-1} = E^P[X_t|Y_{t-1}] = \Phi_t^{X,0}(\psi) + \Phi_t^{X,1}(\psi) X_{t-1},$$
$$\Sigma_{t|t-1} = \Phi_t^{X,1}(\psi) \Sigma_{t-1} \Phi_t^{X,1}(\psi)' + Q_t(\psi),$$

where $\Phi_t^{X,0} = (I - \exp(-K^P \Delta t))\theta^P$, $\Phi_t^{X,1} = \exp(-K^P \Delta t)$, and $Q_t = \int_0^{\Delta t} e^{-K^P s} \Sigma \Sigma' e^{-(K^P)' s} ds$, while Δt is the time between observations.

In the time-t update step, $X_{t|t-1}$ is improved by using the additional information contained in Y_t. We have

$$X_t = E[X_t|Y_t] = X_{t|t-1} + \Sigma_{t|t-1} B(\psi)' F_t^{-1} v_t,$$
$$\Sigma_t = \Sigma_{t|t-1} - \Sigma_{t|t-1} B(\psi)' F_t^{-1} B(\psi) \Sigma_{t|t-1},$$

where

$$v_t = y_t - E[y_t|Y_{t-1}] = y_t - A(\psi) - B(\psi) X_{t|t-1},$$
$$F_t = cov(v_t) = B(\psi) \Sigma_{t|t-1} B(\psi)' + H(\psi),$$
$$H(\psi) = diag(\sigma_\varepsilon^2(\tau_1), \ldots, \sigma_\varepsilon^2(\tau_N)).$$

At this point, the Kalman filter has delivered all ingredients needed to evaluate the Gaussian log likelihood, the prediction-error decomposition of which is

$$\log l(y_1, \ldots, y_T; \psi) = \sum_{t=1}^{T} \Big(-\frac{N}{2} \log(2\pi) - \frac{1}{2} \log|F_t| - \frac{1}{2} v_t' F_t^{-1} v_t \Big),$$

where N is the number of observed yields. We numerically maximize the likelihood with respect to ψ using the Nelder–Mead simplex algorithm. Upon convergence, we obtain standard errors from the estimated covariance matrix,

$$\widehat{\Omega}(\widehat{\psi}) = \frac{1}{T} \Big[\frac{1}{T} \sum_{t=1}^{T} \frac{\partial \log l_t(\widehat{\psi})}{\partial \psi} \frac{\partial \log l_t(\widehat{\psi})}{\partial \psi}' \Big]^{-1},$$

where $\widehat{\psi}$ denotes the estimated model parameters.

This completes the description of the standard Kalman filter. However, in the shadow-rate models, the zero-coupon bond yields are not affine functions of the state variables. Instead, the measurement equation takes the general form

$$y_t = z(X_t; \psi) + \varepsilon_t.$$

In the extended Kalman filter we use, this equation is linearized through a first-order Taylor expansion around the best guess of X_t in the prediction step of the

Kalman filter algorithm. Thus, in the notation introduced above, this best guess is denoted $X_{t|t-1}$ and the approximation is given by

$$z(X_t;\psi)\approx z(X_{t|t-1};\psi)+\frac{\partial z(X_t;\psi)}{\partial X_t}\Big|_{X_t=X_{t|t-1}}(X_t-X_{t|t-1}).$$

Now, by defining[31]

$$A_t(\psi)\equiv z(X_{t|t-1};\psi)-\frac{\partial z(X_t;\psi)}{\partial X_t}\Big|_{X_t=X_{t|t-1}}X_{t|t-1}\quad\text{and}\quad B_t(\psi)\equiv\frac{\partial z(X_t;\psi)}{\partial X_t}\Big|_{X_t=X_{t|t-1}},$$

the measurement equation can be given in an affine form as

$$y_t=A_t(\psi)+B_t(\psi)X_t+\varepsilon_t,$$

and the steps in the algorithm proceeds as previously described.

APPENDIX B: PARAMETER ESTIMATION RESULTS

In this appendix, we report the estimated parameters for the one-, two-, and three-factor standard and shadow-rate models discussed in the main text. Table B1 reports the estimated parameters for both one-factor models. In terms of the Q-dynamics, the very low values of κ^Q imply that the state variable is a level factor. This is also reflected in its very high persistence under the P-dynamics. The estimated mean values θ^P, which are the average levels of the state variable, are about the same in each model. The largest difference between the models is that the B-V(1) model has an estimated factor volatility about 40 percent larger than in the V(1) model.

Tables B2 and B3 report the estimated parameters for the AFNS(2) and B-AFNS(2) models, respectively.

In the AFNS(2) and B-AFNS(2) models, the estimated λ values are low, which indicates that the slope factor in each model operates almost as a level factor for the fit to the cross section of yields. Beyond that, the estimated mean-reversion matrix, mean vector, and volatility matrix share only a few broad similarities such as positive θ_1^P, negative θ_2^P, and negative σ_{21} parameters, but in terms of magnitudes the differences are sizeable.

Tables B4 and B5 contain the estimated parameters for the AFNS(3) and B-AFNS(3) models. With the exception of the estimated λ values and Σ volatility matrices, there are large differences in both signs and magnitudes for most parameters across the two models. Furthermore, the estimated parameters for the level and slope factors in the AFNS(3) models only vaguely resemble the

[31] We calculate these derivatives numerically. See Krippner (2013a) for alternative analytical formulas.

Table B1 Parameter estimates of one-factor models

Parameter	V(1)	B-V(1)
κ^P	0.0311	0.0217
	(0.0831)	(0.1476)
θ^P	0.0097	0.0101
	(0.0102)	(0.0314)
σ	0.0029	0.0042
	(0.0001)	(0.0001)
κ^Q	0.0002	0.0003
	(0.0002)	(0.0002)
θ^Q	14.0501	12.6290
	(10.0754)	(8.4576)
Max log$L$	28,362.97	29,263.60

The estimated parameters are shown for the V(1) and B-V(1) models. The numbers in parentheses are estimated parameter standard deviations.

Table B2 Parameter estimates of the AFNS(2) model

K^P	$K^P_{\cdot,1}$	$K^P_{\cdot,2}$	θ^P	Σ	$\Sigma_{\cdot,1}$	$\Sigma_{\cdot,2}$
$K^P_{1,\cdot}$	−0.5292	−0.5451	0.0682	$\Sigma_{1,\cdot}$	0.0583	0
	(1.3987)	(1.4338)	(0.0344)		(0.0097)	
$K^P_{2,\cdot}$	0.7142	0.6968	−0.0462	$\Sigma_{2,\cdot}$	−0.0590	0.0029
	(1.4338)	(1.4662)	(0.4186)		(0.0097)	(0.0000)

The estimated parameters of the K^P matrix, the θ^P vector, and the Σ matrix are shown for the AFNS(2) model. The associated estimated λ is 0.0179 (0.0031) with maturity measured in years. The numbers in parentheses are estimated parameter standard deviations. The maximum log-likelihood value is 32,186.23.

Table B3 Parameter estimates of the B-AFNS(2) model

K^P	$K^P_{\cdot,1}$	$K^P_{\cdot,2}$	θ^P	Σ	$\Sigma_{\cdot,1}$	$\Sigma_{\cdot,2}$
$K^P_{1,\cdot}$	0.4096	0.5461	0.1111	$\Sigma_{1,\cdot}$	0.0076	0
	(0.2187)	(0.2375)	(0.0781)		(0.0003)	
$K^P_{2,\cdot}$	−0.2273	−0.2925	−0.1018	$\Sigma_{2,\cdot}$	−0.0070	0.0048
	(0.2107)	(0.2435)	(0.0575)		(0.0003)	(0.0001)

The estimated parameters of the K^P matrix, the θ^P vector, and the Σ matrix are shown for the B-AFNS(2) model. The associated estimated λ is 0.1260 (0.0039) with maturity measured in years. The numbers in parentheses are estimated parameter standard deviations. The maximum log-likelihood value is 32,808.21.

Table B4 Parameter estimates of the AFNS(3) model

K^P	$K^P_{\cdot,1}$	$K^P_{\cdot,2}$	$K^P_{\cdot,3}$	θ^P	Σ	$\Sigma_{\cdot,1}$	$\Sigma_{\cdot,2}$	$\Sigma_{\cdot,3}$
$K^P_{1,\cdot}$	2.0515	2.5376	−0.8283	0.0539	$\Sigma_{1,\cdot}$	0.0137	0	0
	(1.1176)	(1.3554)	(0.3924)	(0.1266)		(0.0005)		
$K^P_{2,\cdot}$	−0.7631	−0.8852	0.3825	−0.0466	$\Sigma_{2,\cdot}$	−0.0132	0.0026	0
	(1.0967)	(1.3327)	(0.3831)	(0.0987)		(0.0005)	(0.0001)	
$K^P_{3,\cdot}$	1.5648	2.1032	0.4196	−0.0267	$\Sigma_{3,\cdot}$	−0.0199	−0.0017	0.0147
	(1.6314)	(1.9929)	(0.5450)	(0.0098)		(0.0009)	(0.0004)	(0.0003)

The estimated parameters of the K^P matrix, the θ^P vector, and the Σ matrix are shown for the AFNS(3) model. The associated estimated λ is 0.3918 (0.0044) with maturity measured in years. The numbers in parentheses are estimated parameter standard deviations. The maximum log-likelihood value is 35,469.67.

Table B5 Parameter estimates of the B-AFNS(3) model

K^P	$K^P_{\cdot,1}$	$K^P_{\cdot,2}$	$K^P_{\cdot,3}$	θ^P	Σ	$\Sigma_{\cdot,1}$	$\Sigma_{\cdot,2}$	$\Sigma_{\cdot,3}$
$K^P_{1,\cdot}$	2.0140	3.0510	−1.0411	0.0040	$\Sigma_{1,\cdot}$	0.0211	0	0
	(0.7362)	(1.1116)	(0.3695)	(0.1434)		(0.0006)		
$K^P_{2,\cdot}$	−0.8440	−1.3316	0.4768	0.0352	$\Sigma_{2,\cdot}$	−0.0192	0.0040	0
	(0.7016)	(1.0417)	(0.3244)	(0.3557)		(0.0006)	(0.0001)	
$K^P_{3,\cdot}$	−1.9305	−3.4216	1.1847	0.1118	$\Sigma_{3,\cdot}$	−0.0292	−0.0009	0.0177
	(1.0397)	(1.4122)	(0.5008)	(0.7828)		(0.0009)	(0.0006)	(0.0004)

The estimated parameters of the K^P matrix, the θ^P vector, and the Σ matrix are shown for the B-AFNS(3) model. The associated estimated λ is 0.4896 (0.0043) with maturity measured in years. The numbers in parentheses are estimated parameter standard deviations. The maximum log-likelihood value is 36,520.00.

corresponding parameters in the AFNS(2) models, but this is a common feature when estimating flexible latent factor models such as ours.[32]

Received November 14, 2013; revised February 21, 2014; accepted March 5, 2014.

REFERENCES

Bauer, M. D., and G. D. Rudebusch. 2013. "Monetary Policy Expectations at the Zero Lower Bound." Working Paper 2013-18, Federal Reserve Bank of San Francisco.

Black, F. 1995. Interest Rates as Options. *Journal of Finance* 50: 1371–1376.

Bomfim, A. N. 2003. "'Interest Rates as Options: Assessing the Markets' View of the Liquidity Trap." Working Paper 2003-45, Finance and Economics Discussion Series, Federal Reserve Board, Washington, D.C.

[32]This is part of the reason why CDR recommend focusing on parsimonious specifications of the AFNS models, say, with a diagonal Σ matrix and additional restrictions on K^P as in Christensen, Lopez, and Rudebusch (2010).

Bullard, J. 2012. "Shadow Interest Rates and the Stance of U.S. Monetary Policy." Speech on November 8, 2012, Center for Finance and Accounting Research Annual Corporate Finance Conference, Olin Business School, Washington University, St. Louis.

Chen, R.-R. 1992. Exact Solutions for Futures and European Futures Options on Pure Discount Bonds. *Journal of Financial and Quantitative Analysis* 27: 97–107.

Cheridito, P., D. Filipović, and R. L. Kimmel. 2007. Market Price of Risk Specifications for Affine Models: Theory and Evidence. *Journal of Financial Economics*, 83: 123–170.

Christensen, J. H. E., F. X. Diebold, and G. D. Rudebusch. 2011. The Affine Arbitrage-Free Class of Nelson-Siegel Term Structure Models. *Journal of Econometrics*, 164: 4–20.

Christensen, J. H. E., J. A. Lopez, and G. D. Rudebusch. 2010. Inflation Expectations and Risk Premiums in an Arbitrage-Free Model of Nominal and Real Bond Yields. *Journal of Money, Credit and Banking* 42(suppl.): 143–178.

Christensen, J. H. E., and G. D. Rudebusch. 2013. "Modeling Yields at the Zero Lower Bound: Are Shadow Rates the Solution?." Working Paper 2013-39, Federal Reserve Bank of San Francisco.

Christoffersen, P., C. Dorion, K. Jacobs, and L. Karoui. 2013. "Nonlinear Kalman Filtering in Affine Term Structure Models." Manuscript, Rotman School of Management.

Dai, Q., and K. J. Singleton. 2002. Expectations Puzzles, Time-Varying Risk Premia, and Affine Models of the Term Structure. *Journal of Financial Economics* 63: 415–441.

Diebold, F. X., and G. D. Rudebusch. 2013. *Yield Curve Modeling and Forecasting: The Dynamic Nelson-Siegel Approach*. Princeton, NJ: Princeton University Press.

Duffee, G. R. 2002. Term Premia and Interest Rate Forecasts in Affine Models. *Journal of Finance* 57: 405–443.

Filipović, D., and A. B. Trolle. 2013. The Term Structure of Interbank Risk. *Journal of Financial Economics* 109: 707–733.

Fisher, M., and C. Gilles. 1996. Term Premia in Exponential-Affine Models of the Term Structure. Manuscript, Board of Governors of the Federal Reserve System.

Gorovoi, V., and V. Linetsky. 2004. Black's Model of Interest Rates as Options, Eigenfunction Expansions and Japanese Interest Rates. *Mathematical Finance* 14: 49–78.

Ichiue, H., and Y. Ueno. 2007. Equilibrium Interest Rates and the Yield Curve in a Low Interest Rate Environment. Working Paper 2007-E-18, Bank of Japan.

Ichiue, H., and Y. Ueno. 2013. Estimating Term Premia at the Zero Bound: An Analysis of Japanese, US, and UK Yields. Working Paper 2013-E-08, Bank of Japan.

Kim, D. H., and M. Priebsch. 2013. Estimation of Multi-Factor Shadow-Rate Term Structure Models. Manuscript, Federal Reserve Board, Washington, D.C.

Kim, D. H., and K. J. Singleton. 2012. Term Structure Models and the Zero Bound: An Empirical Investigation of Japanese Yields. *Journal of Econometrics* 170: 32–49.

Krippner, L. 2012. "Modifying Gaussian Term Structure Models when Interest Rates Are Near the Zero Lower Bound." Discussion Paper 2012-02, Reserve Bank of New Zealand.

Krippner, L. 2013a. "A Tractable Framework for Zero-Lower-Bound Gaussian Term Structure Models." Discussion Paper 2013-02, Reserve Bank of New Zealand.

Krippner, L. 2013b. Measuring the Stance of Monetary Policy in Zero Lower Bound Environments. *Economics Letters* 118: 135–138.

Litterman, R., and J. A. Scheinkman. 1991. Common Factors Affecting Bond Returns. *Journal of Fixed Income* 1: 62–74.

Merton, R. C. 1974. On the Pricing of Corporate Debt: The Risk Structure of Interest Rates. *Journal of Finance* 29: 449–470.

Nelson, C. R., and A. F. Siegel. 1987. Parsimonious Modeling of Yield Curves. *Journal of Business* 60: 473–489.

Priebsch, M. 2013. "Computing Arbitrage-Free Yields in Multi-Factor Gaussian Shadow-Rate Term Structure Models." Finance and Economics Discussion Series Working Paper 2013-63, Board of Governors of the Federal Reserve System.

Richard, S. F. 2013. A Non-Linear Macroeconomic Term Structure Model. Manuscript, the Wharton School, University of Pennsylvania.

Ueno, Y., N. Baba, and Y. Sakurai. 2006. "The Use of the Black Model of Interest Rates as Options for Monitoring the JGB Market Expectations." Working Paper 2006-E-15, Bank of Japan.

Vasiček, O. 1977. An Equilibrium Characterization of the Term Structure. *Journal of Financial Economics* 5: 177–188.

Wu, C., and F. Dora Xia. 2013. Measuring the Macroeconomic Impact of Monetary Policy at the Zero Lower Bound. Manuscript, University of California at San Diego.